Tumor Biol. (2016) 37:14903–14914
DOI 10.1007/s13277-016-5392-4

ORIGINAL ARTICLE

Hypoxia-induced NIPP1 activation enhances metastatic potential and predicts poor prognosis in hepatocellular carcinoma

Yun Huang[1] · Yiming Tao[1] · Kuan Hu[1] · Feng Lin[1] · Xinying Li[1] · Tiecheng Feng[1] · Zhi-Ming Wang[1]

Received: 10 June 2016 / Accepted: 9 September 2016 / Published online: 19 September 2016

Abstract Hypoxia is known to promote hepatocellular carcinoma (HCC) invasion and metastasis and nuclear inhibitor of protein phosphatase 1 (NIPP1) overexpression contributes to the malignant phenotype in HCC. The aim of this study was to investigate the role of NIPP1 in HCC development under hypoxia. We first conducted a study with 106 cases to explore the association of NIPP1 and/or enhancer of zeste homolog 2 (EZH2) expression with poor prognosis in HCC. Then additional 352 independent cases were recruited to validate the results in the first stage. Hypoxia was induced by culturing HCC cells in 1 % O_2 or of the treatment with hypoxic agent. The expression levels of NIPP1/EZH2 in both HCC tissues and HCC cell lines were detected by RT-PCR, Western blot, or immunohistochemistry. We also studied the effects of the loss of function of NIPP1 and EZH2 on malignant phenotypes, downstream pathway, and inflammatory factors activities using gene silencing strategy. Overall, we found that NIPP1 and EZH2 were overexpressed in both HCC tissue samples and HCC cell lines. High expression of HIPP1 was associated with poor prognosis and clinicopathological features in patients with advanced HCC. HIPP1 expression positively correlated with the expression of hypoxia marker (carbonic anhydrase IX). Hypoxia induced high expression of NIPP1. NIPP1/EZH2 knockdown in HCC cell lines under hypoxia suppressed the malignant phenotypes, reduced the expression of hypoxia-inducible Factor 1α, downstream molecules of EZH2, and inhibit the activity of inflammatory factors. In conclusion, we found that NIPP1 could be activated by hypoxia and contributed to hypoxia-induced invasive and metastatic potential in HCC.

Keywords Nuclear inhibitor of protein phosphatase 1 · Enhancer of zeste homolog 2 · Hypoxia · Hypoxia-inducible factor 1α · Hepatocellular carcinoma

Introduction

Hepatocellular carcinoma (HCC) is the fifth most common solid tumor around the world [1]. China has a high incidence of HCC, accounting for 55 % new cases of liver cancer worldwide [2]. Moreover, HCC represents the second most frequent cause of cancer-related death in China [2]. Common risk factors for HCC include chronic hepatitis B virus (HBV) and hepatitis C virus (HCV) infections [3], alcoholic cirrhosis, non-alcoholic steatohepatitis, consumption of aflatoxin-contaminated foods, and exposure to other chemical carcinogens [4]. Surgical resection remains the main therapy for the majority of HCC cases. Despite great improvements in surgical skills and perioperative anesthetic management, as well as substantial reduction in the risk of surgery, the 5-year survival rate is still low [5]. Recurrence and metastasis are still key limiting factors in the improvement of survival after surgical excision. Thus, understanding molecular mechanism underlying tumor recurrence and metastasis is essential for effectively combating HCC.

Numerous clinical and basic studies have been performed to explore the mechanism underlying HCC invasion and metastasis. Although great progresses have been made, the mechanisms were still ambiguous. Accumulating evidence

Electronic supplementary material The online version of this article (doi:10.1007/s13277-016-5392-4) contains supplementary material, which is available to authorized users.

✉ Zhi-Ming Wang
zhimingwang66@sina.com

[1] Department of Hepatobiliary Surgery, Xiangya Hospital, Central South University, 87 Xiangya Road, Changsha, Hunan 410078, China

indicated that apart from the conventional factors associated with uninodular or multinodular HCC, inflammation and changes in the tumor microenvironment also largely contribute to the development of HCC [7]. Hypoxia, one of the most common stresses in the tumor microenvironment, results from overwhelming growth of tumor and inadequate blood supply to tumor cells [7]. It has great influence on tumor cells and microenvironment in a variety of malignancies including HCC [8]. The implication of hypoxia in tumor development has been explored since the early 1920s [9]. Recent studies have paid attention to the effects of hypoxia on tumor neovascularization and inflammation in carcinogenesis [10].

Enhancer of zeste homolog 2 (EZH2), belonging to the polycomb group genes (PcG) family, regulates cell growth and survival through catalyzing histone H3-Lys27 trimethylation (H3K27me3) and mediating epigenetic silencing of gene expression [11, 12]. Overexpression of EZH2 has been found in liver cancer [13], and it has been demonstrated to be involved in tumor cell differentiation and cell invasion in various cancers including HCC [14]. Previous study indicated that nuclear inhibitor of protein phosphatase 1 (NIPP1) plays an important role in EZH2-mediated gene expression modulation [15]. NIPP1, together with nuclear type 1 protein phosphatase (PP1), has been shown to be implicated in malignant phenotype of liver cancer [16]. However, whether NIPP1/EZH2 plays roles in HCC tumor microenvironment, especially under hypoxia, is still unknown.

Thus, the present study was performed to explore the role and regulatory mechanism of NIPP1/EZH2 in the development of HCC under hypoxia. Firstly, we investigated the expression levels of NIPP1/EZH2 in both HCC tissues and cell lines and the prognostic values of the two protein molecules in HCC. Secondly, we further explored the expression of NIPP1/EZH2 in HCC under hypoxia and the regulatory mechanism through silencing NIPP1/EZH2 expression. Our study helps to understand the regulatory mechanisms in tumor microenvironment, especially under hypoxia.

Material and methods

Cell lines

HepG2, SMCC7721, Bel7404, Hep3B, and MHCC97-L cell line (low invasive potential human HCC cell lines), HCCLM3 cell line (high invasive potential human HCC cell line), and immortalized human hepatocyte line L02 were used in this study. MHCC97-L and HCCLM3 cell line were purchased from Zhongshan Hospital, affiliated Fudan University in Shanghai. HepG2, SMCC7721, Bel7404, Hep3B, and L02 cells were obtained from Cell Institute of Xiangya School of Medicine, Central South University. All cells were cultured in high glucose Dulbecco's modified Eagle's medium (DMEM, Gibco, Carlsbad, CA, USA) supplemented with 10 % fetal bovine serum (Gibco, Carlsbad, CA, USA) and maintained at 37 °C in a moist atmosphere containing 5 % CO_2 in air.

Hypoxia treatment

SMCC7721 and HCCLM3 cell lines in exponential growth were seeded in serum-free culture for 24 h and exposed to hypoxia in a hypoxic chamber (1 % O_2, 94 % N_2, and 5 % CO_2) for indicated duration.

In addition, hypoxic condition induced by cobalt chloride ($CoCl_2$) and deferoxamine (DFO) was also established in our study. Briefly, SMCC7721 and HCCLM3 cell lines were grown to subconfluence of 60–70 % in normoxia and treated with $CoCl_2$ (100 μm) or DFO (100 μm). Then cells were further cultured for indicated duration.

HCC tissue samples

Patients

HCC tissue samples used in our study were collected with informed consent from patients who underwent radical resection surgery for HCC at the Department of Surgery of Xiangya School of Medicine, Central South University. This study was approved by the research ethics committee of Xiangya School of Medicine, Central South University. All recruited patients had confirmed primary HCC. A total of 106 pairs of tumorous and adjacent nontumorous liver tissues were collected from patients from January 2010 to June 2010 were used to explore the relationship of NIPP1 and/or EZH2 expression with prognosis in HCC in the first stage. Additional 352 independent cases recruited between February 2009 and December 2010 were used in the validation cohort study. The response rate was approximately 85 % for HCC patients. The basic information and exclusion criteria were shown in supplementary information.

Clinicopathologic features and follow-up

Patients from both study and validation stage underwent a clinical examination. Clinicopathologic features were obtained from patients, including hepatitis B virus surface antigen (HBsAg), albumin level, alpha fetal protein level, liver function (assessed by Child-Pugh classification), liver cirrhosis (with or without), tumor diameter (the largest diameter of tumor), number of tumors (single tumor or multiple tumors), satellite nodules (with or without), tumor venous invasion (with or without), tumor capsule (with or without), tumor differentiation (defined by the Edmondson grading system), liquefactive necrosis (with or without), and tumor staging [defined by both the International Union Against Cancer TNM

classification system and the Barcelona Clinic Liver Cancer (BCLC) scoring system].

Quantitative reverse transcription-PCR

Total RNA from tissue samples or cells was extracted using the TRIzol reagent (Invitrogen, Carlsbad, CA, USA) according to the provided protocol. RNA quantity and quality were determined by using spectrophotometry at 260 nm and electrophoresis by 1 % agarose gel, respectively. Then RNA was reverse-transcribed using the Prime Script reagent RT kit (Takara, Tokyo, Japan) following the manufacturer's instruction. Then primers for *NIPP1* and *EZH2* were designed and synthesized by Takara (shown in supplementary information); *β-actin* was used as an internal control to normalize the expression of *NIPP1* and *EZH2*. Real-time PCR was conducted on the ABI 7900 Prism HT (Applied Biosystems, Foster City, CA, USA) using Maxima SYBR Green/ROX qPCR Master Mix kit (Fermentas Inc., St. Leon-Rot, Germany). Real-time PCR data were analyzed using $^{\triangle\triangle}$Ct method.

Western blot

Tissue samples or cells were first homogenized with lysis buffer. Then lysates were isolated by centrifugation. Protein samples were quantified using a standard bicinchoninic acid assay (Pierce, Rockford, IL, USA). After quantification, proteins were run and separated on a 10 % sodium dodecyl sulfate-polyacrylamide gel electrophoresis (SDS-PAGE) and transferred onto a polyvinylidene difluoride membrane. Then membranes were incubated in 5 % milk in 0.1 % Tris-buffered saline-Tween 20 (TBST) at room temperature for 2 h. Afterwards, membranes were incubated with specific primary antibodies at 4 °C overnight. The antibodies were displayed in supplementary information. Subsequently, membranes were incubated with horseradish peroxidase (HRP)-conjugated anti-mouse or rabbit secondary antibodies (Abcam, Cambridge, MA, USA) at dilution of 1:5000. Membranes incubated with mouse anti-human α-tubulin or β-actin primary antibody were set as loading controls. Finally, membranes were washed and visualized by enhanced chemiluminescene system (GE Healthcare, Piscataway, NJ, USA).

Immunohistochemistry

Tumor tissue samples collected from patients were fixed in 4 % paraformaldehyde, embedded in paraffin, and cut into 4–5-μm sections for further analysis. For immunostaining, sections were incubated with specific primary antibodies (supplementary information) at 4 °C overnight, followed by incubated in biotin-labeled anti-mouse or anti-rabbit secondary antibody (1: 5000, Abcam, Cambridge, MA, USA) at room temperature for 30 min. Then all slides were incubated with streptavidin-conjugated with peroxidase (Zymed, San Francisco, CA, USA) for 20 min at 37 °C. Next, 3,3-diaminobenzidine was used for the color development and hematoxylin was used for counterstaining. Slides, omitting primary antibodies, were used as negative controls.

Immunostaining for NIPP1, EZH2, and CA IX proteins was assessed by two independent investigators who were both blinded to clinical data of patients. At least 5 random and non-overlapping fields at ×100 magnification were evaluated to determine the expression level (high or low) of NIPP1, EZH2, and CA IX by integrating both area and intensity of immunostaining. The method for evaluation was shown in supplementary information.

Small interfering RNAs and transfection

NIPP1, HIF-1α, and HIF-2α siRNAs were designed using OligoEngine software (OligoEngine, Inc., Seattle, USA) and synthesized by Shanghai Genechem Co., Ltd. (Shanghai, China). Then NIPP1, HIF-1α, and HIF-2α siRNAs and negative-control siRNAs were transfected into HCCLM3 and SMCC-7721 cell lines using Lipofectamine 2000 (Invitrogen, Carlsbad, CA, USA) following the manufacturer's instructions. Six hours after transfection, the transfection medium was replaced by complete medium. All experiments were conducted 24 h after transfection.

Detection for cell proliferation, cell invasion, cell migration, and small GTPase activity

Clonogenic assay for cell proliferation, wound healing assay for cell invasion, and transwell assay for cell migration were performed using SMCC7721 and HCCLM3 cell lines. Small GTPase activity was detected by measuring the GTP-bound Cdc42 level using both HCCLM3 and SMCC-7721 cell lines. The procedures for all these experiments were shown in supplementary information.

Enzyme-linked immunosorbent assay

The activities of interleukin-6 (IL-6) and interleukin-8 (IL-8) were detected using enzyme-linked immunosorbent assay (ELISA). Briefly, HCCLM3 and SMCC-7721 cell lines were seeded into anti-IL-6 or IL-8 primary antibody-coated polystyrene plates. Each plate contained blank controls, negative controls, and positive controls. Then all wells were incubated with HRP-conjugated antibodies and color development was realized by addition of 3, 3′, 5, 5′,-tetramethylbenzidine (TMB) solution. The reaction was terminated by the addition

of sulfuric acid, and spectrophotometry measurements were made at 450 nm.

Statistical analysis

Statistical analysis was performed using SPSS 20.0 software (SPSS, Inc., Chicago, IL, USA). Continuous variables were presented as mean ± standard deviation (SD) and compared using independent *t* test or Mann-Whitney *U* test. Categorical variables were compared using χ^2 test. Overall survival rate and recurrence-free survival rate for patients were calculated using Kaplan-Meier method. Univariate and multivariate Cox regression analysis was used to evaluate the association of risk factors with the prognosis of HCC. A value of $P < 0.05$ was considered statistically significant.

Results

Overexpression of NIPP1/EZH2 correlates with poor prognosis of HCC

In the first stage of the study, we first detected the difference in the expression of NIPP1/EZH2 between 106 HCC tumor tissues and paired adjacent nontumorous liver tissues. Both NIPP1 and EZH2 expression levels were significantly unregulated in the HCC biopsies compared to the paired adjacent nontumorous liver tissue in both mRNA level and protein level ($P < 0.05$, Fig. 1a, b). In addition, the expression of NIPP1 significantly positively correlated with the expression of EZH2 ($P < 0.001$, Fig. 1c). In the first stage, we also explored the association of NIPP1 and EZH2 expression levels

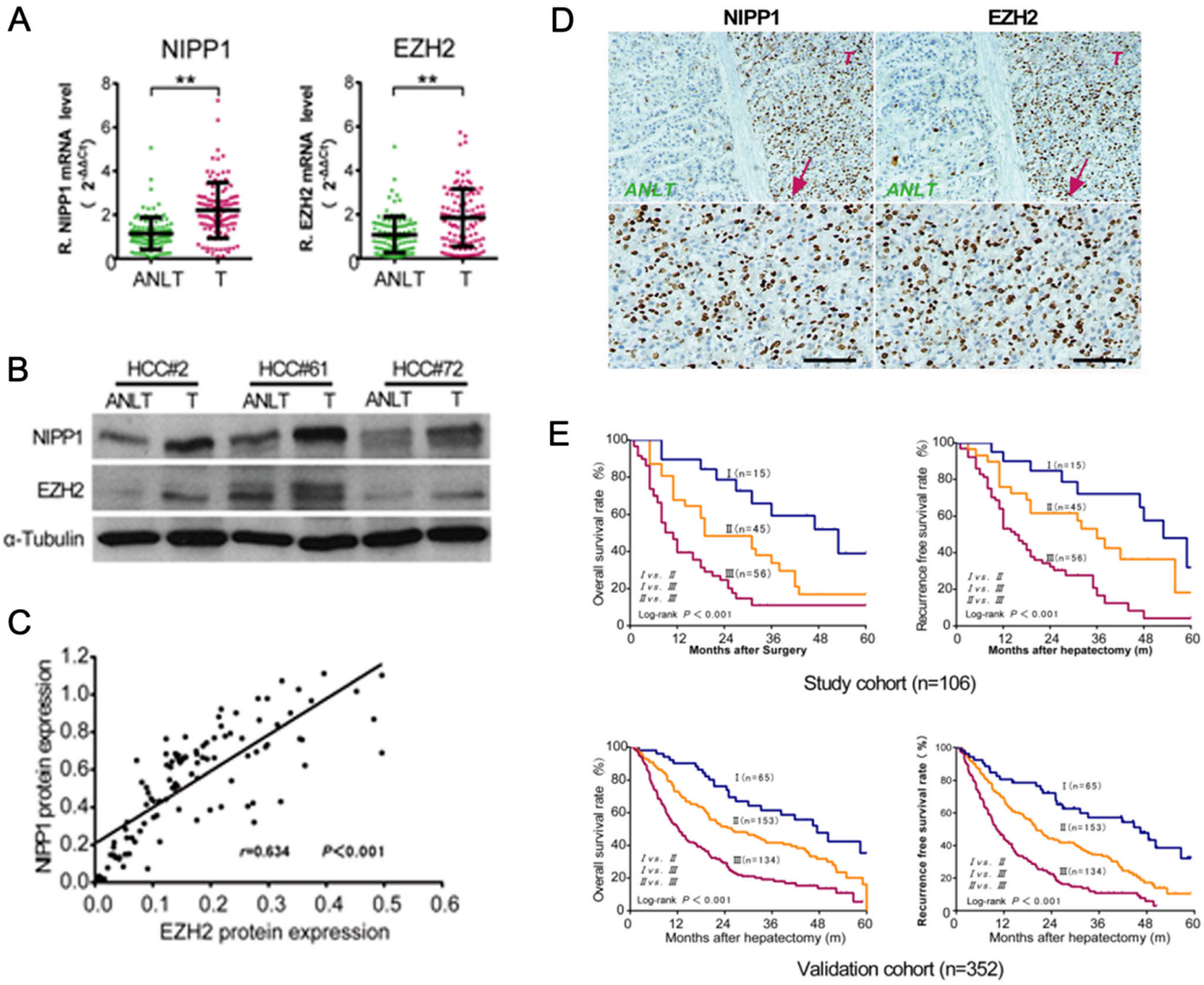

Fig. 1 Overexpression of NIPP1/EZH2 in human HCC tissues. **a** NIPP1 and EZH2 mRNA expression level of the sample tissues was determined by qRT-PCR and normalized to that of β-actin. **b** NIPP1 and EZH2 protein expression of the sample tissue was determined by Western blot assay. Tubulin was used as the loading control. **c** Correlation analysis of NIPP1 expression with EZH2 expression. **d** Immunohistochemical staining for both NIPP1 and EZH2 in human HCC tissue samples. **e** Kaplan-Meier analysis of recurrence-free survival (*left panel*) and overall survival (*right panel*) of HCC patients with overexpression of NIPP1 and EZH2

with several clinicopathologic features in HCC patients. As expected, the expression levels of both NIPP1 and EZH2 were significantly positively correlated with the number of tumor nodules, tumor differentiation, tumor venous invasion, liquefactive necrosis as well as tumor staging ($P < 0.05$, Table 1). Moreover, patients with high expression levels of NIPP1 and EZH2 had significantly shorter survival than those with low expression levels, respectively (Fig. 1e).

Additional 352 independent cases were recruited to validate the association of NIPP1 and EZH2 expression with survival in HCC. Overall, 279 of 352 cases (85.8 %) and 268 of 352 cases (76.4 %) had tumors with high expression levels of NIPP1 and EZH2, respectively (Fig. 1d). Then we performed both univariate and multivariate Cox regression analysis to explore the risk factors associated with tumor recurrence or overall survival. As presented in Table 2, both NIPP1 and EZH2 are independent predictors of overall survival [relative risk (RR), 2.837, $P < 0.001$; RR, 2.673, $P < 0.001$] as well as tumor recurrence (RR, 3.268, $P < 0.001$; RR, 2.854, $P < 0.001$) in patients with HCC (Table 2). We further confirmed the correlation between NIPP1/EZH2 expression and several clinicopathologic features in patients with HCC. Consistently, both NIPP1 and EZH2 expression were highly expressed in patients with invasive tumors such as presence of satellites nodules and tumor venous invasion and poor differentiation (data not shown). Furthermore, patients were redivided into three groups when considering both NIPP1 and EZH2 expression together. As shown in Table 2 and Fig. 1e, patients with both NIPP1 and EZH2 overexpression had shorter overall survival and recurrence-free survival ($P < 0.001$).

NIPP1 expression significantly positively related to the expression of CA IX in HCC

The relationship between NIPP1 and CA IX (a reliable marker for hypoxia) has been explored in our study. First, high expression of CA IX in HCC tumor samples was detected in 220 of 352 cases (62.5 %) by immunohistochemistry. The remaining 132 cases were found with CA IX low expression. The immunoreaction of NIPP1 was also detected among 352 cases, among which 73 cases were with low expression and

Table 1 Correlation of NIPP1 and EZH2 expression with clinicopathologic features collected from 106 patients with HCC in exploratory research

Clinicopathologic features		Number	Expression level		*P* value	
			NIPP1	EZH2	NIPP1	EZH2
Age (years)	≤60	68	3.25 ± 0.19	0.69 ± 0.45		
	> 60	38	2.12 ± 0.17	1.12 ± 0.09	0.854	0.692
Sex	Male	91	2.96 ± 0.13	0.86 ± 0.12		
	Female	15	1.86 ± 0.27	1.47 ± 0.21	0.387	0.886
HBsAg	Negative	8	2.34 ± 0.45	0.97 ± 0.35		
	Positive	98	2.13 ± 0.22	1.09 ± 0.19	0.393	0.578
Albumin level (g/L)	≤35	12	1.98 ± 0.31	0.87 ± 0.16		
	>35	94	1.75 ± 0.09	0.69 ± 0.11	0.561	0.437
AFP level (ng/mL)	≤20	30	2.12 ± 0.27	0.99 ± 0.24		
	>20	96	2.58 ± 0.34	1.15 ± 0.17	0.169	0.095
Child-Pugh classification	A	97	1.98 ± 0.22	0.79 ± 0.26		
	B	9	1.66 ± 0.27	0.91 ± 0.19	0.476	0.685
Liver cirrhosis	Without	14	2.01 ± 0.17	0.89 ± 0.26		
	With	92	2.31 ± 0.23	0.91 ± 0.17	0.089	0.102
Tumor capsule	Without	63	2.75 ± 0.15	0.93 ± 0.14		
	With	43	2.96 ± 0.11	0.83 ± 0.22	0.063	0.079
Tumor diameter (cm)	≤5	39	2.67 ± 0.29	0.76 ± 0.29		
	>5	67	3.85 ± 0.48	0.89 ± 0.14	0.066	0.091
Number of tumors	Single tumor	52	2.07 ± 0.38	0.45 ± 0.17		
	Multiple tumors	54	2.76 ± 0.41	1.09 ± 0.12	0.028	0.033
Satellite nodules	Without	41	1.85 ± 0.12	0.74 ± 0.14		
	With	65	3.43 ± 0.29	1.02 ± 0.09	0.021	0.009
Tumor venous invasion	Without	61	2.01 ± 0.23	0.88 ± 0.12		
	With	45	2.75 ± 0.19	1.07 ± 0.15	<0.001	<0.001
Tumor differentiation	I–II	71	2.78 ± 0.13	1.05 ± 0.42		
	III–IV	35	3.21 ± 0.34	1.12 ± 0.33	0.012	0.005
Tumor necrosis	Without	44	2.26 ± 0.14	0.72 ± 0.28		
	With	62	3.15 ± 0.29	0.95 ± 0.35	0.009	0.014
Tumor staging	A–B	80	2.13 ± 0.22	0.97 ± 0.16		
(BCLC scoring system)	C	26	3.52 ± 0.19	1.03 ± 0.37	0.031	0.045
Tumor staging	I-II	85	1.75 ± 0.36	0.74 ± 0.23		
(TNM classification system)	III	21	2.89 ± 0.37	1.01 ± 0.14	0.012	0.024

HCC hepatocellular carcinoma, *HBsAg* hepatitis B virus surface antigen, *AFP* alpha fetal protein, *BCLC* Barcelona Clinic Liver Cancer, *TNM* tumor node metastasis

Table 2 Univariate and multivariate Cox regression analysis of risk factors associated with OS and TTR in 352 cases

Variables	TTR				OS			
	Univariate	Multivariate			Univariate	Multivariate		
	P	RR	95 % CI	*P* value	*P*	RR	95 % CI	*P*
HBsAg (positive vs. negative)	0.789	NA			0.641	NA		
Albumin level (g/L) (≤35 vs. >35 g/L)	0.478	NA			0.625	NA		
Child-Pugh classification (A vs. B)	0.028	NA			0.042	NA		
Liver cirrhosis (with vs. without)	0.035	NA			0.026	NA		
AFP (≤20 vs. >20 ng/mL)	0.015	1.421	0.935–1.894	NS	0.027	1.398	0.857–1.786	NS
Tumor diameter (≤5 vs. >5 cm)	0.026	1.084	0.897–1.632	NS	0.017	1.021	0.836–1.549	NS
Number of tumors (single tumor vs. multiple tumors)	0.019	1.689	1.135–1.886	0.006	0.008	1.645	1.123–1.739	0.003
Tumor capsule (with vs. without)	0.032	1.116	0.786–1.458	NS	0.027	NA		
Satellites nodules (with vs. without)	0.003	1.794	1.136–2.064	0.012	0.001	1.766	1.115–2.043	<0.001
Tumor venous invasion(with vs. without)	<0.001	2.417	1.568–3.054	<0.001	<0.001	2.407	1.527–3.017	<0.001
Tumor differentiation (I/II vs. III/IV)	<0.001	1.324	0.851–1.735	NS	<0.001	1.314	0.843–1.646	NS
Tumor necrosis (with vs. without)	<0.001	2.629	1.225–6.532	<0.001	<0.001	2.554	2.357–4.931	<0.001
Tumor staging (TNM classification system) (I/II vs. III)	0.031	1.542	1.034–1.874	0.042	0.024	1.532	1.029–1.796	0.017
Tumor staging (BCLC scoring system) (A/B vs. C)	0.026	1.576	1.098–1.753	<0.001	0.021	1.536	1.065–1.743	0.012
NIPP1 expression (low vs. high)	<0.001	3.268	1.427–6.828	<0.001	<0.001	2.837	2.328–4.102	<0.001
EZH2 expression (low vs. high)	<0.001	2.854	2.357–5.231	<0.001	<0.001	2.673	1.395–4.736	<0.001
Combined NIPP1 and EZH2 expression								
II vs. I	0.001	2.831	1.348–4.963	<0.001	<0.001	2.785	1.593–4.957	<0.001
III vs. I	<0.001	6.321	2.576–11.013	<0.001	<0.001	8.123	2.842–10.973	<0.001
III vs. II	<0.001	3.715	1.596–7.229	<0.001	<0.001	4.331	2.013–6.982	<0.001

TTR time for tumor recurrence, *OS* overall survival, *HBsAg* hepatitis B virus surface antigen, *AFP* alpha fetal protein, *BCLC* Barcelona Clinic Liver Cancer, *TNM* tumor node metastasis, *RR* relative risk, *95 % CI* 95 % confidence interval, *NA* not available, *NS* not significant

I, NIPP1 low expression combined with EZH2 low expression; II, NIPP1 high expression combined with EZH2 low expression or NIPP1 low expression combined with EZH2 high expression; III, NIPP1 high expression combined with EZH2 high expression

279 cases with high expression (Table 3). According to the results in Supplementary Fig. 1, cases with high NIPP1 expression had significantly higher density of intratumoral CA IX, indicating that there is a correlation between the expression of NIPP1 and CA IX. Then we performed subgroup analysis to explore the expression relationship between NIPP1 and CA IX. In CA IX low expression group, NIPP1 expression was not significantly correlated with clinicopathologic features of patients. However, in CA IX high expression group, cases with high NIPP1 expression had poorer prognosis such as the development of multiple tumors, presence of tumor venous invasion, satellites nodules and liquefactive necrosis, as well as poor tumor differentiation and high tumor staging ($P < 0.05$). These results indicated that CA IX overexpression induced by hypoxia could upregulate the expression of NIPP1.

Overexpression of NIPP1/EZH2 in HCC cell lines

Moreover, we also explored the expression of NIPP1/EZH2 in HCC cell lines including HepG2, SMCC7721, Bel7404, Hep3B, MHCC97-L, and HCCLM3 cell lines, while NIPP1/EZH2 expression in L02 was set as controls. Following the results in Supplementary Fig. 2, expression of both NIPP1 and EZH2 was higher in HCC cell lines than that in L02 cell lines at mRNA and protein level. There was a statistically significant difference in SMCC-7721 and HCCLM3 cell lines based on the results from RT-PCR ($P < 0.05$).

Hypoxia-induced NIPP1 overexpression in HCC cells

HCC cell lines (HepG2, Hep3B, SMCC-7721, and HCCLM3) were cultured under hypoxia, and the expression of NIPP1 in these cell lines was detected using RT-PCR and Western blot. The results were shown in Supplementary Fig. 3. Hypoxia led to increased expression of NIPP1 in a time-dependent manner. When cells were cultured under hypoxia for 12 h, expression of NIPP1 reached its peak at both mRNA and protein level in all four HCC lines.

Table 3 Correlation analysis of NIPP1 and CA IX expression with clinicopathologic features in 352 cases with HCC

Clinicopathologic features		Total cases (n = 352)			CA IX low expression (normoxia)			CA IX low expression (hypoxia)		
		NIPP1 low expression (%)	NIPP1 high expression (%)	P	NIPP1 low expression (%)	NIPP1 high expression (%)	P	NIPP1 low expression (%)	NIPP1 high expression (%)	P
Age (years)	≤60	42 (21.6)	162 (79.4)	0.935	28 (35.4)	51 (64.6)	0.962	14 (11.2)	111 (88.8)	0.834
	>60	31 (20.9)	117 (79.1)		19 (35.8)	34 (64.2)		12 (12.6)	83 (87.4)	
Sex	Male	61 (19.6)	251 (80.4)	0.125	40 (35.7)	72 (64.3)	0.951	21 (10.5)	179 (89.5)	0.069
	Female	12 (30.0)	28 (70.0)		7 (35.0)	13 (65.0)		5 (25.0)	15 (75.0)	
Child-Pugh classification	A	71 (20.5)	276 (79.5)	0.285[a]	46 (35.4)	84 (64.6)	0.999[a]	25 (11.5)	192 (88.5)	0.316[a]
	B	2 (40.0)	3 (60.0)		1 (50.0)	1 (50.0)		1 (33.3)	2 (66.7)	
AFP level (ng/mL)	≤20	38 (20.9)	144 (79.1)	0.946	25 (30.5)	57 (69.5)	0.136	13 (13.0)	87 (87.0)	0.678
	>20	35 (20.6)	135 (79.4)		22 (44.0)	28 (56.0)		13 (10.8)	107 (89.2)	
Liver cirrhosis	Without	11 (33.3)	22 (66.7)	0.061	9 (37.5)	15 (62.5)	0.818	2 (22.2)	7 (77.8)	0.288
	With	62 (19.4)	257 (80.6)		38 (35.2)	70 (64.8)		24 (11.4)	187 (88.6)	
Tumor diameter (cm)	≤5	36 (25.7)	104 (74.3)	0.080	30 (35.7)	54 (64.3)	0.973	6 (10.7)	50 (89.3)	0.767
	>5	37 (17.5)	175 (82.5)		17 (35.4)	31 (64.6)		20 (12.2)	144 (87.8)	
Number of tumors	Single	58 (30.1)	135 (69.9)	<0.001	39 (39.4)	60 (60.6)	0.115	19 (20.2)	75 (79.8)	0.001
	Multiple	15 (9.4)	144 (90.6)		8 (24.2)	25 (75.8)		7 (5.6)	119 (94.4)	
Tumor capsule	Without	41 (22.8)	139 (77.2)	0.334	32 (37.2)	54 (62.8)	0.704	9 (9.6)	85 (90.4)	0.407
	With	32 (18.6)	140 (81.4)		15 (32.6)	31 (67.4)		17 (13.5)	109 (86.5)	
Satellite nodules	Without	43 (27.9)	111 (72.1)	0.003	33 (31.7)	71 (68.3)	0.080	10 (20.0)	40 (80.0)	0.041
	With	30 (15.2)	168 (84.8)		14 (50.0)	14 (50.0)		16 (9.4)	154 (90.6)	
Tumor venous invasion	Without	60 (26.4)	167 (73.6)	<0.001	42 (36.2)	74 (63.8)	0.787	18 (32.7)	37 (67.3)	<0.001
	With	13 (10.4)	112 (89.6)		5 (31.3)	11 (68.8)		8 (4.8)	157 (95.2)	
Tumor differentiation	I-II	62 (24.2)	194 (75.8)	0.009	38 (35.2)	70 (64.8)	0.818	24 (16.2)	124 (83.8)	0.003
	III	11 (11.5)	85 (88.5)		9 (37.5)	15 (62.5)		2 (2.8)	70 (97.2)	
Tumor necrosis	Without	54 (32.9)	110 (67.1)	<0.001	37 (37.0)	63 (63.0)	0.673	17 (26.6)	47 (73.4)	<0.001
	With	19 (10.1)	169 (89.9)		10 (31.3)	22 (68.7)		9 (5.8)	147 (94.2)	
Tumor staging (BCLC scoring system)	A-B	60 (24.3)	196 (76.6)	0.041	36 (34.3)	69 (65.7)	0.653	24 (15.9)	127 (84.1)	0.006
	C	13 (13.5)	83 (86.5)		11 (40.7)	16 (59.3)		2 (2.9)	67 (97.1)	
Tumor staging (TNM classification system)	I-II	65 (25.2)	193 (74.8)	0.001	42 (35.0)	78 (65.0)	0.754	23 (16.3)	118 (83.7)	0.005
	III-IV	8 (8.5)	86 (91.5)		5 (41.7)	7 (58.3)		3 (3.8)	76 (96.2)	

HCC hepatocellular carcinoma, *AFP* alpha fetal protein, *BCLC* Barcelona Clinic Liver Cancer, *TNM* tumor node metastasis [a] Comparison performed with Fisher' exact test

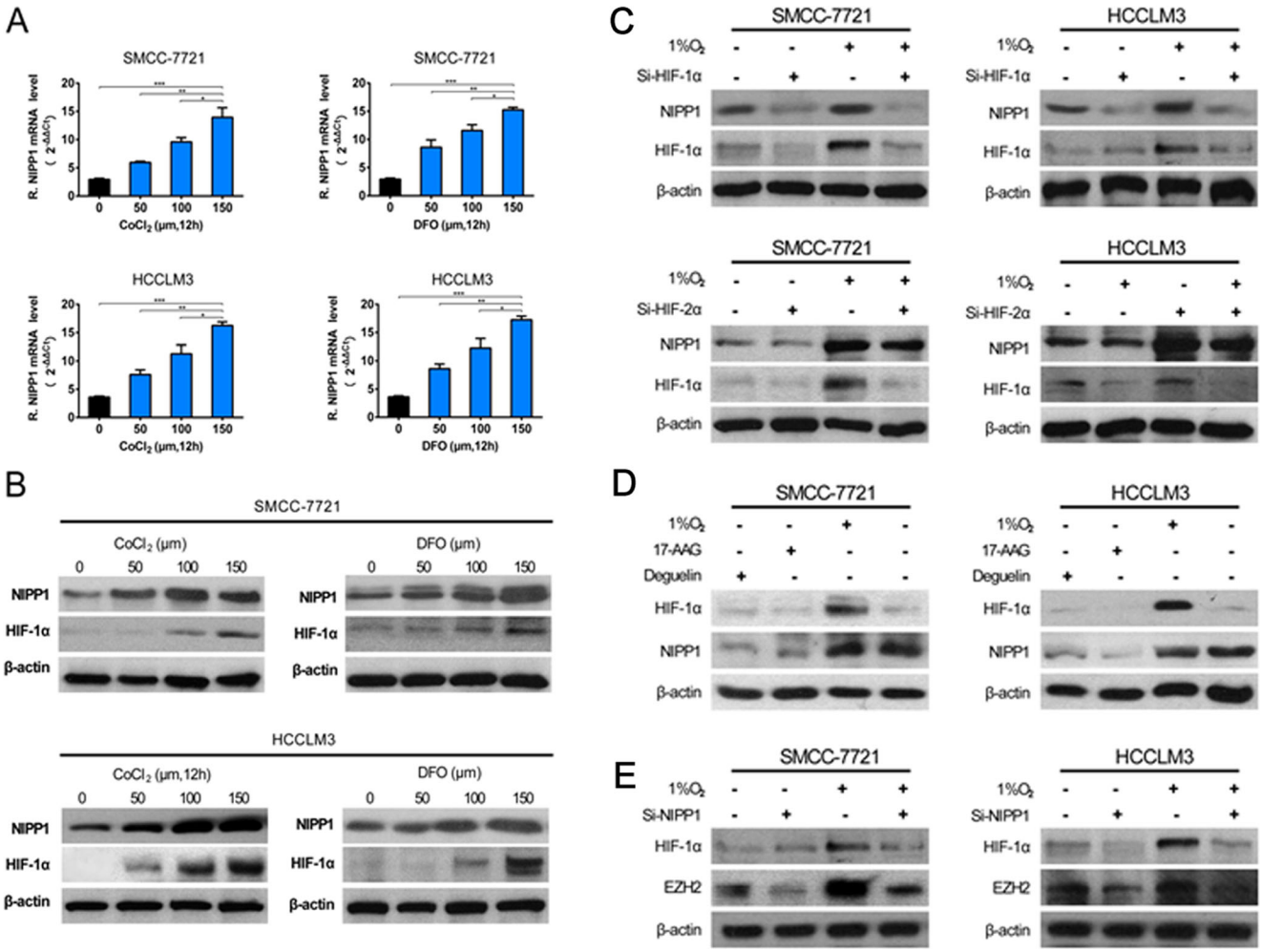

Fig. 2 Regulatory relationships between NIPP1 and HIF-1α in HCC after exposing hypoxia. **a** NIPP1 mRNA expression level was upregulated after addition of HIF-1α activators ($CoCl_2$ and DFO) into HCC cell lines. The longer the exposure was, the greater the influence became (*$p < 0.05$, **$p < 0.01$, **$p < 0.005$). **b** The expression of NIPP1 was upregulated at protein level after addition of HIF-1α activators ($CoCl_2$ and DFO) into HCC cell lines. **c** Silencing HIF-1α expression by siRNAs (*upper figure*) induced downregulation of NIPP1 expression at protein level ($p < 0.05$), while silencing HIF-2α (*lower figure*) exerts no similar results ($p > 0.05$). **d** Addition of HIF-1α inhibitor (deguelin and 17-AAG) induced downregulation of NIPP1 expression at protein level ($p < 0.05$). **e** Silencing HIF-1α expression by siRNAs induced downregulation of EZH2 expression at protein level ($p < 0.05$)

Regulatory mechanism of NIPP1 involved in HCC cells after hypoxia treatment

To reveal the molecular mechanism of NIPP1 overexpression in hypoxic HCC cells, hypoxia was induced by the addition of $CoCl_2$ or DFO, both of which were HIF-1α activators. RT-PCR and Western blot revealed that the expression levels of HIF-1α and NIPP1 were upregulated with the increasing dose of $CoCl_2$ or DFO (Fig. 2a, b, $P < 0.05$). These results demonstrated that NIPP1 overexpression in hypoxic HCC cells might be positively regulated by HIF-1α.

Then the expression of both HIF-1α and HIF-2α in hypoxic HCC cells was interfered using their corresponding siRNAs. NIPP1 expression was significantly decreased after knockdown of HIF-1α, but not HIF-2α (Fig. 2c). The similar results were obtained after the addition of HIF-1α inhibitors deguelin and 17-AAG (Fig. 2d). Additionally, we also downregulated the expression of NIPP1 using siRNAs, and both HIF-1α and EZH2 expression were significantly decreased based on the results from Western blot (Fig. 2e). These results indicated that there is a mutual regulation relationship between HIF-1α and NIPP1, and EZH2 is the downstream factor of NIPP1 in HCC cell, while exposed to hypoxia.

Downregulation of NIPP1 under hypoxia is responsible for the relief of HCC malignant behaviors

To find the direct evidence that hypoxia-induced NIPP1 overexpression is involved in tumor growth, invasion, and metastasis, a series of cell experiments were performed. Following the results from clonogenic assay in the study, NIPP1 silencing in both SMCC-7721 and HCCLM3 cell lines suppressed cell

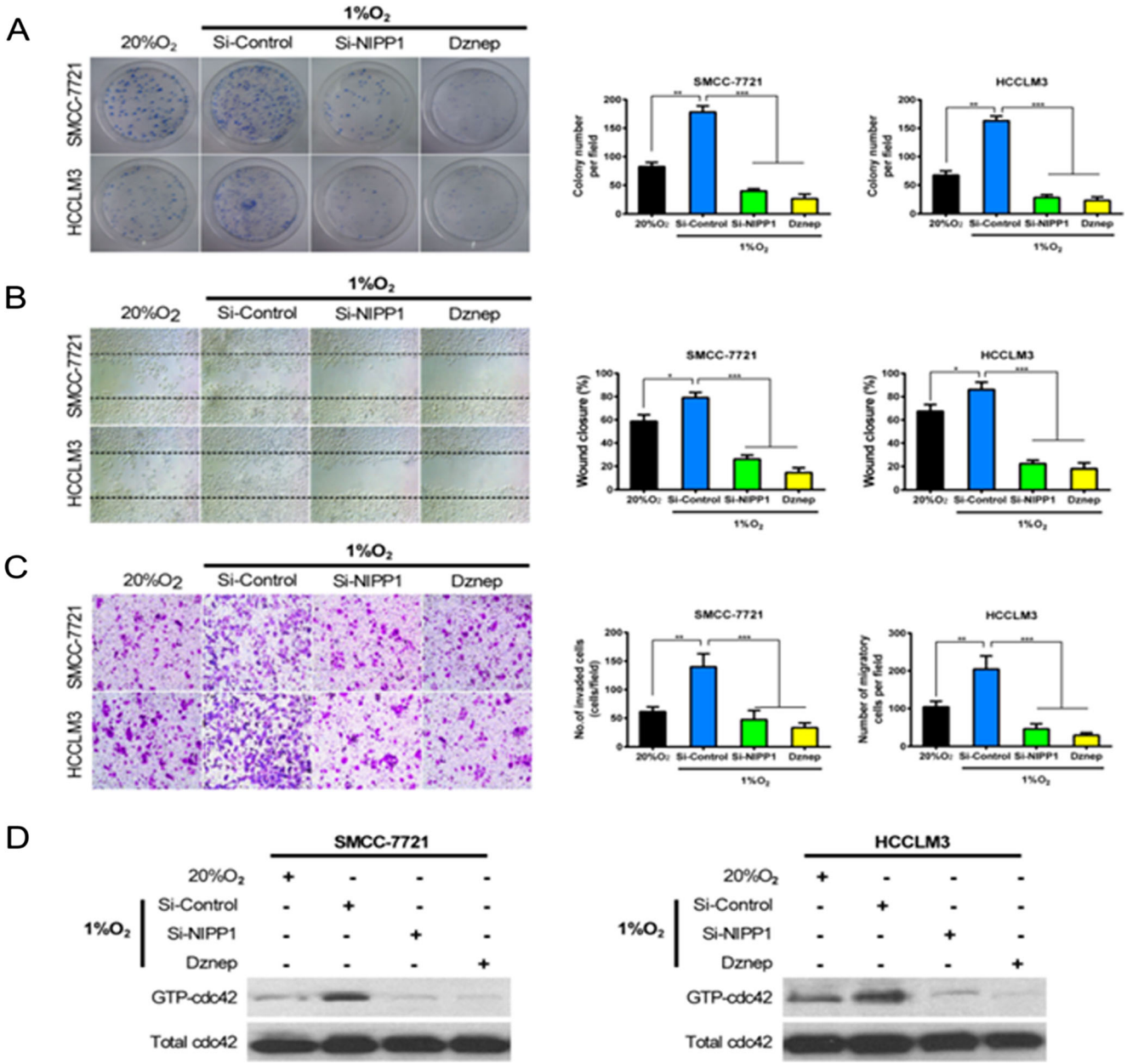

Fig. 3 Silencing NIPP1 expression by siRNAs affects malignant behavior of HCC cells under hypoxia. **a** Clonogenic assay for tumor cell proliferation showed downregulated proliferation ability of HCC cell lines after silencing NIPP1 in hypoxic environment. **b** Wound healing assay showed downregulated invasiveness of HCC cell lines after silencing NIPP1 in hypoxic environment. **c** Transwell assay showed downregulated migration ability of HCC cell lines after silencing NIPP1 in hypoxic environment. **d** Western blot assay showed silencing of NIPP1 induced change in GTP-bound Cdc 42 expression level (*$p < 0.05$, **$p < 0.01$, **$p < 0.005$)

proliferation and growth ($P < 0.05$, Fig. 3a). Moreover, reduced cell invasion (wound healing assay) and migration ability (transwell assay) were also observed in HCC cells after inhibiting NIPP1 expression ($P < 0.05$, Fig. 3b, c). We also detected the changes of small GTPase activity in HCC cells. GTP-bound cdc42 activity was obviously disturbed after silencing NIPP1 expression in HCC cells ($P < 0.05$, Fig. 3d). The EZH2 inhibitor, 3-Deazaneplanocin A (Dznep), was used as positive controls. All these results demonstrated that downregulation of NIPP1 could inhibit cell proliferation, motility, and invasion, thus suppressing tumor growth and metastasis.

Downregulation of NIPP1/EZH2 expression reduced the expression of several downstream molecules in HCC cells after hypoxia treatment

In order to directly demonstrate the important role of NIPP1/EZH2 in hypoxic HCC cell, we also monitored

the alterations in the activities of several downstream molecules after *NIPP1* or *EZH2* silencing. We found that the addition of NIPP1 siRNA or Dznep could decrease the expression of H3K27me3, Netrin-1, p65, HDAC1, and PP1 and p-Akt in hypoxic HCC cells (Fig. 4a). Furthermore, inhibition of NIPP1/EZH2 could also downregulate IL-6 and IL-8 level secreted from HCC cell after hypoxia treatment ($P < 0.05$, Fig. 4b).

Discussion

Recurrence and metastasis occurred frequently in patients with HCC, with a 2-year rate of 50 % and a 5-year rate of 70–80 %, respectively. The high rates of tumor recurrence and metastasis for in HCC patients are attributed to the high invasive and metastatic ability of HCC cells. Therefore, understanding the underlying molecular mechanism of cell invasion

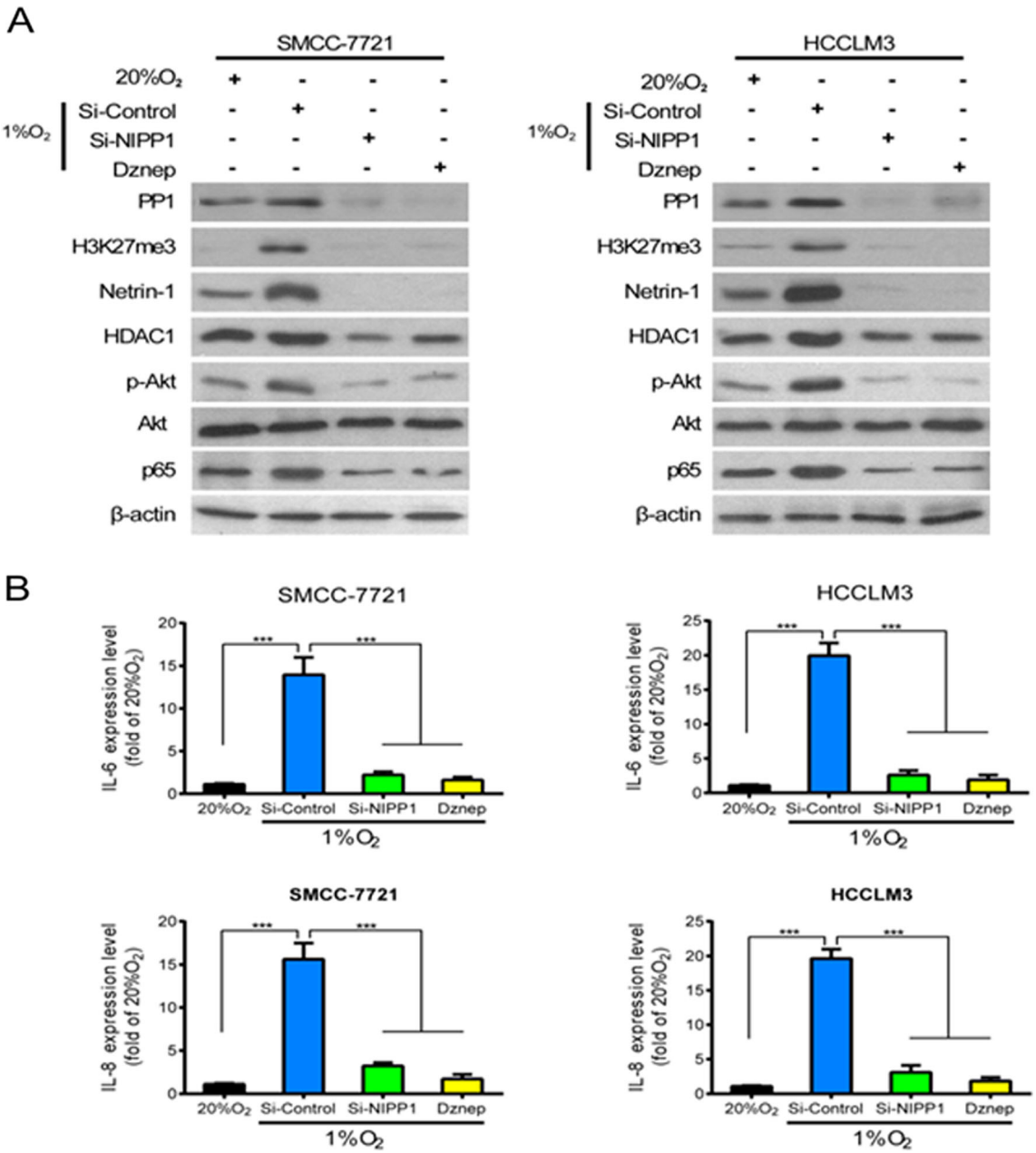

Fig. 4 Downregulation of NIPP1 and EZH2 decrease the expression of EZH2 downstream molecules (**a**) and inflammatory molecule activity (**b**) in HCC cells under hypoxia

and metastasis in HCC is essential for exploring new biomarkers and therapeutic targets for this disease. In our study, we found that NIPP1/EZH2 overexpressed in HCC tissues as well as in cell lines which was associated with poor prognosis of HCC. Additionally, we have found that NIPP1 expression was significant associated with tumor staging, tumor differentiation, tumor nodules, and tumor venous invasion. All these results indicated that NIPP1 is involved in tumor invasion and metastasis in HCC. Previous study indicated that EZH2, a target gene of miRNA124, regulates ROCK signaling pathway and promotes cell invasion and metastasis in HCC. The expression of EZH2 in tumor cells has been considered a prognostic factor for cancers. During tumor angiogenesis, vascular endothelial growth factor produced through paracrine directly stimulates the endothelial cells to increase the expression of EZH2. Then EZH2 mediates epigenetic silencing of vasohibinl (an inhibitor for angiogenesis) expression through regulating H3K27me3 modification. Moreover, histone modification is the key epigenetic factor controlling Wnt/β-catenin pathways. Thus, EZH2 overexpression-induced β-catenin accumulation causes the excessive growth of tumor cell. EZH2 has been shown to be regulated by NIPP1. It is speculated that NIPPI might function as an upstream regulator of EZH2 to participate in tumor growth and invasion.

Hypoxia is one of the most pervasive microenvironment stresses in solid tumors, and it occurred frequently during HCC development. Our study found that NIPP1 expression was positively correlated with CA IX, a type of metalloproteinase that is commonly detected in various types of tumors. High expression of CA IX is believed to be related to the hypoxic microenvironment in tumors, and CA IX is considered as a reliable marker for hypoxia, which further proved our hypothesis that NIPP1 might play a crucial role in the tumorogenesis under hypoxic environment.

HIF-1α is the most widely expressed in tumor hypoxic microenvironment and the most studied transcriptional factor. HIF-1α prompts tumor cells to adapt to the hypoxic environment, and it also alters the characteristics of tumor cells to make them more invasive and metastatic. Moreover, HIF-1α can also regulate the expression of several inflammatory factors and chemokines and modifying tumor microenviroment, consequentially facilitating tumor survival. We observed the correlation between the expression of HIF-1α and NIPP1 in HCC. Hypoxic cells were induced by the addition of $CoCl_2$ or DFO, both of which were HIF-1α activators. We found that activated HIF-1α could upregulate NIPP1 expression. Meanwhile, silencing NIPP1 expression under hypoxia could decrease the expression of both HIF-1α and EZH2. These results demonstrated that there was a mutual regulation mechanism between HIF-1α and NIPP1 in hypoxic tumor microenvironment. Moreover, we have found that all downstream factors including H3K27me3, Netrin-1, p65, HDAC1, and PP1 and p-Akt were downregulated after silencing either EZH2 or NIPP1 expression in HCC under hypoxia. These results indicated that NIPP1 promoted HCC development under hypoxia by regulating the expression of EZH2. In addition, NIPP1/EZH2 also regulate the activity of IL-6 and IL-8. However, the pathogenesis and signaling pathway of the tumorogenesis of HCC are far more complicated than expected. Further, well-designed studies are warranted to reveal the underlying mechanisms of HCC carcinogenesis.

In conclusion, this work shows that NIPP1/EZH2 expression can be a reliable prognostic factor for HCC. NIPP1 promotes tumor growth, invasion, and metastasis through activating EZH2 and downstream signaling pathways as well as several hypoxic markers under hypoxia in HCC. Our results advance the understanding the underlying mechanism of tumor environment influencing HCC development.

Acknowledgments This study was supported by the grants from the National Nature Science Foundation of China (no. 81372631). We wish to express our warm thanks to Fenghe (Shanghai) Information Technology Co., Ltd. Their ideas and help gave a valuable added dimension to our research.

Compliance with ethical standards

Conflicts of interest The authors declare no conflicts of interest.

References

1. Siegel R, Naishadham D, Jemal A. Cancer statistics, 2013. CA Cancer J Clin. 2013;63:11–30.
2. Chen W, Zheng R, Baade PD, Zhang S, Zeng H, Bray F, Jemal A, XQ Y, He J. Cancer statistics in China, 2015. CA Cancer J Clin. 2016;66:115–32.
3. Dhanasekaran R, Bandoh S, Roberts LR. Molecular pathogenesis of hepatocellular carcinoma and impact of therapeutic advances. F1000Res. 2016; doi: 10.12688/f1000research.6946.1.
4. Nordenstedt H, White DL, El-Serag HB. The changing pattern of epidemiology in hepatocellular carcinoma. Dig Liver Dis. 2010;42(Suppl 3):S206–14.
5. Zhong JH, Ke Y, Wang YY, Li LQ. Liver resection for patients with hepatocellular carcinoma and macrovascular invasion, multiple tumours, or portal hypertension. Gut. 2015;64:520–1.
6. Joyce JA, Pollard JW. Microenvironmental regulation of metastasis. Nat Rev Cancer. 2009;9:239–52.

7. Shay JE, Simon MC. Hypoxia-inducible factors: crosstalk between inflammation and metabolism. Semin Cell Dev Biol. 2012;23:389–94.
8. Kong B, Cheng T, Wu W, Regel I, Raulefs S, Friess H, Erkan M, Esposito I, Kleeff J, Michalski CW. Hypoxia-induced endoplasmic reticulum stress characterizes a necrotic phenotype of pancreatic cancer. Oncotarget. 2015;6:32154–60.
9. Bartrons R, Caro J. Hypoxia, glucose metabolism and the warburg's effect. J Bioenerg Biomembr. 2007;39:223–9.
10. Antonioli L, Blandizzi C, Pacher P, Haskó G. Immunity, inflammation and cancer: a leading role for adenosine. Nat Rev Cancer. 2013;13:842–57.
11. Debeb BG, Gong Y, Atkinson RL, Sneige N, Huo L, Gonzalez-Angulo AM, Hung MC, Valero V, Ueno NT, Woodward WA. Ezh2 expression correlates with locoregional recurrence after radiation in inflammatory breast cancer. J Exp Clin Cancer Res. 2014;33:58.
12. Fu Y, Chen J, Pang B, Li C, Zhao J, Shen K. Ezh2-induced h3k27me3 is associated with epigenetic repression of the arhi tumor-suppressor gene in ovarian cancer. Cell Biochem Biophys. 2015;71:105–12.
13. Zheng F, Liao YJ, Cai MY, Liu YH, Liu TH, Chen SP, Bian XW, Guan XY, Lin MC, Zeng YX. The putative tumour suppressor microrna-124 modulates hepatocellular carcinoma cell aggressiveness by repressing rock2 and ezh2. Gut. 2012;61:278–89.
14. Cheng AS, Lau SS, Chen Y, Kondo Y, Li MS, Feng H, Ching AK, Cheung KF, Wong HK, Tong JH. Ezh2-mediated concordant repression of wnt antagonists promotes β-catenin–dependent hepatocarcinogenesis. Cancer Res. 2011;71:4028–39.
15. Nuytten M, Beke L, Van Eynde A, Ceulemans H, Beullens M, Van Hummelen P, Fuks F, Bollen M. The transcriptional repressor nipp1 is an essential player in ezh2-mediated gene silencing. Oncogene. 2008;27:1449–60.
16. Nam JS, Ino Y, Sakamoto M, Hirohashi S. Src family kinase inhibitor pp2 restores the e-cadherin/catenin cell adhesion system in human cancer cells and reduces cancer metastasis. Clin Cancer Res. 2002;8:2430–6.